Identification and Assignment of Base Pairs in the "Tuned Helix" of Intact and Ribonuclease T1 Cleavage Fragments of Wheat Germ Ribosomal 5S RNA via 500-MHz Proton Homonuclear Overhauser Enhancements†

Shi-Jiang Li‡ and Alan G. Marshall*,§

Department of Biochemistry, The Ohio State University, Columbus, Ohio 43210

Received July 17, 1985; Revised Manuscript Received November 14, 1985

ABSTRACT: Wheat germ has been chosen as a representative eukaryote for study of ribosomal 5S RNA secondary structure. Proton homonuclear Overhauser enhancements (NOE's) at 500 MHz for the hydrogen-bonded base-pair protons in the 10–15 ppm region are used to establish the identity (A·U, G·C, or G·U) and base-pair sequence (e.g., G·C-A·U-C·G) within a given helical segment. Assignment of that segment to particular base pairs in the secondary structure is based upon NOE's conducted at different temperatures (to determine which signals "melt" together), variation of salt conditions (to produce differential chemical shifts in order to better distinguish components of an unresolved spectral envelope), and isolation and purification of RNase T1 cleavage fragments (in order to reduce the spectrum to just a few base pairs). The NOE patterns for the RNase T1 fragments are the same as in the intact 5S RNA, supporting the assumption that structural features of this region in the intact 5S RNA are preserved in the fragment. Chemical shifts predicted from ring current induced effects for a proposed base-pair sequence are then compared to experimental chemical shifts. By these methods, a portion of the "tuned helix" segment (namely, the base-pair sequence $C_{18}G_{60}$-$A_{19}U_{59}$-$C_{20}G_{58}$) is demonstrated spectroscopically for the first time in any 5S RNA. The tuned helix and common arm segments are less stable than the rest of the molecule. Variation of sodium and magnesium levels reveals multiple configurations of the wheat germ 5S RNA in solution.

Worldwide interest in the proposed universal structure and function of the 5S RNA component of the protein biosynthesis process has led to the determination of 238 primary nucleotide sequences for 5S RNAs from five groups: eubacteria, plastids, mitochondria, archebacteria, and eukaryotes (Erdman et al., 1985). In contrast to the cloverleaf secondary structure for tRNA, which was evident as soon as the first tRNA primary nucleotide sequence was available (Holley, 1965), the 5S RNA secondary structure remains controversial 18 years after the first 5S RNA (from *Escherichia coli*) was sequenced by Brownlee et al. (1967). Not only is 5S RNA about 50% larger than tRNA but also the lack of information about 5S RNA function precludes many of the sorts of structural inferences that resulted from studies of tRNA function. For example, although the conserved GTΨC of tRNAs is Watson–Crick complementary to the conserved GAAC of 5S RNAs, 5S RNA remains functional for protein synthesis even after the GAAC segment has been excised (Pace et al., 1982; Zagorska et al., 1984). The functional nonexchangeability between prokaryotic 5S RNA and eukaryotic 5S RNA renders the problem even harder (Wrede & Erdmann, 1973; Bellemare, 1973).

More than a dozen secondary structural models for 5S RNA have been based upon three major approaches previously applied to tRNAs: comparative sequence analysis (Fox & Woese, 1975; Studnicka et al., 1981; Leuhrsen & Fox, 1981; Pieler & Erdmann, 1982; Delihas & Anderson, 1982; de Wachter et al., 1982; Mackay et al., 1982), chemical modification (Peattie & Gibert, 1980; Woese et al., 1980; Lewis & Doty, 1970; Soot et al., 1974; Brownlee et al., 1968; Jordan, 1971; Vigne et al., 1973; Ross & Brimacombe, 1979), and physical measurements (Osterberg et al., 1976; Luoma & Marshall, 1978a,b; Burns et al., 1980; Matveev et al., 1982; Burkey et al., 1983; Kime & Moore, 1983a,b; Chang et al., 1984; Li et al., 1984b; Kime, 1984a,b; Li & Marshall, 1985). In spite of the voluminous literature on 5S RNAs, a consensus secondary structure has yet to be demonstrated directly. Four-stem and three-stem secondary structures adapted to the primary nucleotide sequence of wheat germ (*Triticum aestivum*) 5S RNA are shown in Figure 1.

In 1971, Kearns et al. (1971a,b) demonstrated that tRNA in H_2O exhibited a large number of hydrogen-bonded imino resonances in the 10–15 ppm downfield region of the proton Fourier transform nuclear magnetic resonance (FT/NMR) spectrum. About a year later, similar (although much less well resolved) resonances were observed from *E. coli* 5S RNA (Wong et al., 1972). Since that time, highly effective water-nulling excitation methods (Redfield et al., 1975; Roth et al., 1980) and homonuclear Overhauser enhancement (NOE) techniques (Johnston & Redfield, 1978) have made it possible to identify (A·U, G·C, G·U, and tertiary pairs), sequence (e.g., A·U followed by G·C etc.), and assign to their correct primary sequence positions virtually all of the secondary and tertiary base pairs in several tRNAs (Johnston & Redfield, 1981; Hare & Reid, 1982a,b; Heerschap et al., 1983a,b). Similar techniques have recently been applied to the elucidation of secondary base pairing in ribosomal 5S RNA from a Gram-negative bacterium, *E. coli* (Kime & Moore, 1983a,b; Kime et al., 1984; Kime, 1984a,b), and a Gram-positive bacterium, *Bacillus subtilis* (Chang & Marshall, 1986). In order to avoid the ambiguities resulting from extensive peak overlap in the 10–15 ppm spectral region in which the base-pair hydrogen-bond proton signals are found, Kime and Moore isolated and examined an RNase A resistant fragment of *E.*

† This work was supported by grants (to A.G.M.) from the U.S. Public Health Service (NIH 1 R01 GM-29274 and NIH 1 S10 RR-01458) and The Ohio State University.

‡ Present address: NMR Research, Johns Hopkins Medical Institute, Baltimore, MD 21205.

§ A.G.M. is also a member of the Department of Chemistry.

0006-2960/86/0425-3673$01.50/0

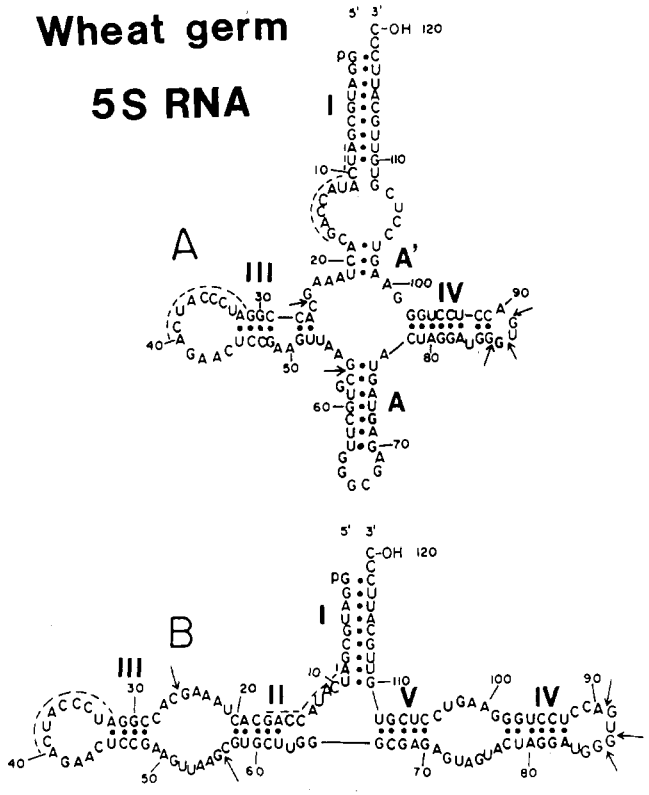

FIGURE 1: Proposed secondary base-pairing schemes for 5S RNA, adapted to the primary nucleotide sequence of wheat germ 5S RNA. (A) Cloverleaf model (Luoma & Marshall, 1978a,b); (B) three-stem model (Luehrsen & Fox, 1981). Both models share segments I, III, and IV and differ in the base pairing in the middle of the primary sequence.

coli 5S RNA to detect segments assigned to the molecular stem and prokaryotic loop of proposed universal base-pairing schemes for 5S RNA (Fox & Woese, 1975; Luoma & Marshall, 1978a,b). However, the regions which differ between different proposed base-pairing schemes (e.g., helix II and helix III in the Fox and Woese model of Figure 1) have not yet been assigned.

In order to resolve this controversy, we decided to apply FT/NMR techniques to wheat germ 5S RNA and its RNase T1 cleavage fragments. 5S RNA from wheat germ cytosol was chosen as a representative eukaryote, because plants and fungi are approximately equally divergent from the evolutionary path leading up to vertebrate animals. In the course of their determination of the primary base sequence of wheat germ 5S RNA, Barber and Nichols (1978) identified RNase T1 first-order cleavage sites at the G residues in positions 86, 87, and/or 89. Therefore, we undertook to isolate and purify the RNase T1 resistant cleavage fragment extending from position 1 to position 86, 87, or 89 of wheat germ 5S RNA. This fragment should eliminate the overlapping imino proton resonances arising from the already observed stem helix of 5S RNA and simplify the direct observation of the base pairs in the remainder of the molecule. Because no one approach is sufficient to solve a problem of this complexity, we have found it necessary to apply additional structural or environmental perturbations (e.g., variation in temperature and/or salt conditions) as well as ring current arguments to aid in enumeration, identification, sequencing, and assignment of base pairs.

Materials and Methods

Wheat Germ 5S RNA. Wheat germ (*Triticum aestivum*) was generously provided by International Multifoods (Co-

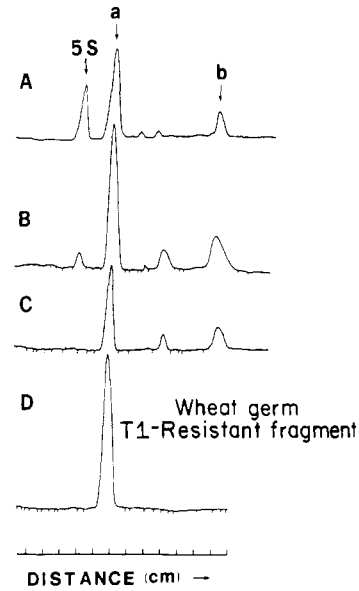

FIGURE 2: Electrophoresis gel scans (550-nm absorbance vs. distance) for production and isolation of RNase T1 cleavage fragments of wheat germ 5S RNA. Scans A, B, and C correspond to RNase T1 digestion at 0 °C for 47, 107, and 137 min, respectively. Components a and b are complementary fragments whose molecular weights add to give the molecular weight of native 5S RNA. Scan D is for fragment a from mixture C after purification via Sephadex G-75 gel filtration chromatography.

lumbus, OH). 5S RNA was isolated and purified via phenol/sodium dodecyl sulfate (SDS) extraction, DE-32 ion-exchange chromatography, and Sephadex G-75 gel filtration as described by Li et al. (1984a).

RNase T1 Cleavage Fragments. To obtain uniform cleavage and high-yield recovery of RNase T1 cleavage fragments of wheat germ 5S RNA, enzymatic digestion was performed at several enzyme concentrations, 5S RNA concentrations, buffer compositions, temperatures, and reaction periods (see Figure 2). Best results were obtained with 3.5 μL of RNase T1 (350 units from Boehringer Mannheim) per milligram of 5S RNA (1 mg/mL) at 0 °C. Wheat germ 5S RNA was dissolved in a solution containing 10 mM tris(hydroxymethyl)aminomethane (Tris) base/0.3 M NaCl at pH 7.0. The reaction was allowed to proceed for 137 min to give complete cleavage at the first-order sites (Figure 2C). Complete cleavage at the first-order sites of wheat germ (WG) 5S RNA is important in obtaining high yield for separation and purification of the RNase T1 resistant cleavage fragment. The reaction was stopped by addition of an equal volume of 5% SDS. Phenol extraction was employed twice to remove RNase T1, and the 5S RNA fragment was recovered from the aqueous supernate by precipitation with 2.5 volumes of cold (−20 °C) ethanol.

Purification of RNase T1 Cleavage Fragments. Preparative-scale separation of RNA fragments from the RNase T1 digest precipitate was achieved via Sephadex G-75 gel filtration chromatography (150 × 2.5 cm) in 4 M urea, 50 mM NaCl, 1 mM ethylenediaminetetraacetic acid (EDTA), and 10 mM Tris base, pH 7.0 at room temperature. The absence of UV hyperchromism (i.e., increase in A_{260} on heating from room temperature to 80 °C; not shown) showed that ≥4 M urea provides denaturing buffer conditions. Thus, the digestion fragments in this buffer are completely separated as single strands without base stacking or base pairing at room temperature. The eluted fractions of the sample cannot be precipitated by ethanol in the presence of 4 M urea. Urea was therefore removed by dialysis against 10 mM Tris base/100

mM NaCl, pH 7.0, and RNA fragments could then be recovered from the urea-free solution via cold ethanol precipitation.

Gel Electrophoresis. The purified RNase T1 cleavage fragments were examined by gel electrophoresis (Li et al., 1984) under denaturing conditions. The gel composition was 2 mL of TBE solution (1.0 M Tris–borate/20 mM EDTA, pH 8.3), 4 mL of monomer [acrylamide/bis(acrylamide) = 38%/2%], 10 g of urea, 7 mg of ammonium persulfate, 30 μL of *N,N,N′,N′*-tetramethylethylenediamine (TEMED), and 6.7 mL of water. The results are shown in Figure 2.

NMR Samples. (A) Intact Wheat Germ 5S RNA. NMR samples of intact WG RNA were prepared in three different buffers. First, all samples were dissolved in a solution containing 10 mM EDTA/10 mM sodium cacodylate at pH 7.0, and dialyzed twice against the same buffer at a volume ratio of 1:500 for 4 h. The samples were then dialyzed 3 times against water at a volume ratio of 1:1000 for 3 h and lyophilized. The lyophilized sample was dissolved in the three different buffers which all contain 10 mM sodium cacodylate and 95%/5% H_2O/D_2O, pH 7.0, to which 100 mM NaCl, 10 mM $MgCl_2$ (buffer A), 100 mM NaCl only (buffer B), 10 $MgCl_2$ only (buffer C), or no NaCl or $MgCl_2$ (buffer D) was added. The concentration of each sample was determined as described by Li and Marshall (1985). RNA concentrations were (A) 30, (B) 35, (C) 26, and (D) 24 mg/mL.

(B) RNase T1 Cleavage Fragments. NMR samples of RNase T1 cleavage fragments were prepared as described above, except that the fragment-lyophilized powder was dissolved in buffer B. To renature this fragment, a dissolved sample was heated in a water bath at 58 °C for 5 min and cooled slowly (30 min). The total amount of RNase T1 resistant fragment was 148 A_{260} units in 0.4 mL. An NMR sample of the common arm fragment was prepared as above, for 105 A_{260} units in 0.4 mL. The isolation and purification of the common arm fragment will be described elsewhere.

NMR Spectroscopy. All spectra were obtained at 11.75 T (500 MHz for ^1H) with a Bruker AM-500 spectrometer unless otherwise specified. The NMR signals were produced by a modified Redfield 21412 pulse sequence (Redfield & Kunz, 1975) with alternate delay acquisition (ADA) (Roth et al., 1980) in order to suppress the H_2O signal (factor of ca. 35000) and give a flatter base line (Chang & Marshall, 1986). 4K data sets (16 bit/word per transient; 24 bit/word in the accumulated transient) were acquired in about 0.16 s. Total acquisition cycle time was 0.8 s; on the basis of independent determination (not shown), the longest T_1 relaxation time was 70 ms. Minor base-line corrections were performed. Sample temperature was calibrated from independent measurements of the chemical shift of methanol and ethylene glycol (Raiford et al., 1979; van Geet, 1970). Downfield shifts are defined as positive, and chemical shifts are defined relative to an H_2O chemical shift of 4.78 ppm. Proton homonuclear Overhauser enhancement (NOE) experiments were performed by 0.3-s preirradiation of the resonance of interest with phase cycling procedures described elsewhere (Chang & Marshall, 1986). Each displayed NOE (difference) spectrum was based on time-domain subtraction of 8000 on-resonance from 8000 off-resonance scans. The decoupler power was within a few decibels of 30 dB below 0.2 W, according to the T_1 of a given peak, the degree of overlap with nearby peaks, and the degree of diffusion of spin polarization from one base-pair proton to another. NOE's were unaffected either by changing the carrier frequency from 12.0 to 15.0 ppm or by increasing the preirradiation period from 0.3 to 0.6 s.

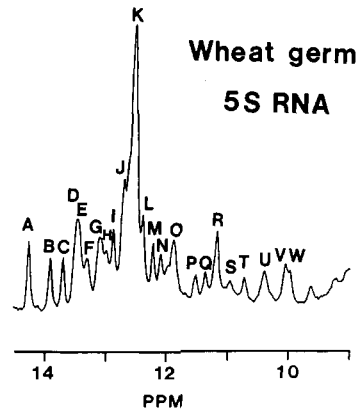

FIGURE 3: 500-MHz low-field ^1H NMR spectrum of wheat germ 5S RNA (35 mg/mL) at 23 °C in buffer B (10 mM sodium cacodylate, 0.1 M NaCl, and 1.0 mM EDTA, pH 7.0, in 95:5 H_2O/D_2O after complete removal of Mg^{2+} ion). The spectrum has been resolution enhanced by Lorentz-to-Gauss conversion. The peaks are labeled from A to W for convenience in discussion.

Results and Discussion

Number of Base Pairs in Intact Wheat Germ 5S RNA. The downfield 500-MHz ^1H FT/NMR spectrum of wheat germ 5S RNA is shown in Figure 3. Because the hydrogen-bond base-pair imino protons give FT/NMR resonances located 10–15 ppm downfield from 4,4-dimethyl-4-sila-1-pentanesulfonic acid (DSS), one might expect to be able to determine the total number of base pairs in an RNA by simple integration of the ^1H intensity in that spectral region. Such estimates are made difficult by several factors. First, even with the Redfield 21412 excitation and alternate delay acquisition, it is difficult to obtain a flat base line because of the residual signal from H_2O. When, as in the present data, the base-line curvature is not very severe, it is permissible to flatten the residual curvature by fitting the base line to a polynomial and subtracting out that curve. Second, the nonflat power spectrum of a Redfield-type pulse sequence further complicates comparison of peak areas. Third, the large number of base pairs in 5S RNA leads to severe overlap in this spectral region (see peak K in Figure 3). The best integration is therefore achieved by simulating the spectrum by superposing the minimum number of Lorentzian (or Gaussian, depending on the experimental line shape) peaks of variable position but equal width and height required to match the experimental spectrum. When applied to the spectrum in Figure 3, such a simulation gives a total base-pair number of about 35.

Although such a procedure corrects for peak overlap, it can still give incorrect base-pair estimates because the relative peak areas may not be proportional to the numbers of base-pair imino protons, due to variation in exchange rate between different base-pair protons and H_2O. Yet another problem is that some resonances in this region may arise from non-Watson–Crick base pairs, e.g., ring NH protons (as for G·U pairs) or exocyclic amino protons involving in hydrogen bonding of other non-Watson–Crick base pairs (as for guanosine, cytosine, and adenine). In support of this point, Hasnoot et al. (1980) have shown that some protons in the molecular interior (e.g., nonpaired G's and U's) may be buried so deep that they cannot exchange with water molecules. Variation in observed peak intensities arising from the detection cyclic period $\leq T_1$ can be eliminated (as in our case) by selecting a repetition period that is long compared to T_1. A final problem is that if 5S RNA in solution can exhibit two or more conformations with interconversion lifetimes longer than a few seconds, then the same base-pair proton from two

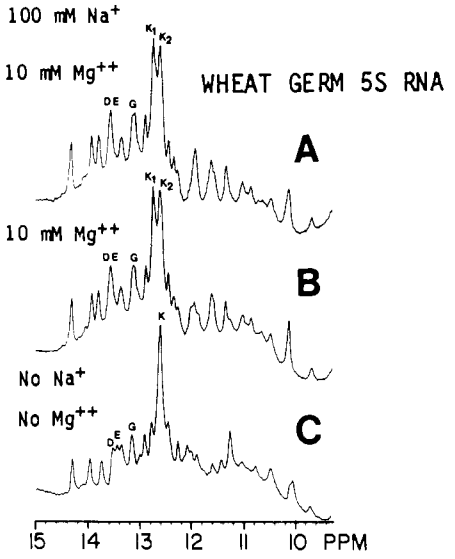

FIGURE 4: Use of salt-induced shifts to resolve overlapping resonances in the downfield ^1H NMR spectrum of intact wheat germ 5S RNA. (A) 30 mg/mL RNA in Buffer A; (B) 26 mg/mL RNA in buffer C; (C) 24 mg/mL RNA in buffer D. Removal of Na^+ and Mg^{2+} (bottom spectrum) resolves peaks D and E. Addition of either Mg^{2+} (middle spectrum) or Na^+ and Mg^{2+} (top spectrum) resolves peak K into two peaks. Numerous salt-induced changes in the 10–12 ppm region suggest that the solution conformation of wheat germ 5S RNA may change significantly according to Na^+ and Mg^{2+} concentrations.

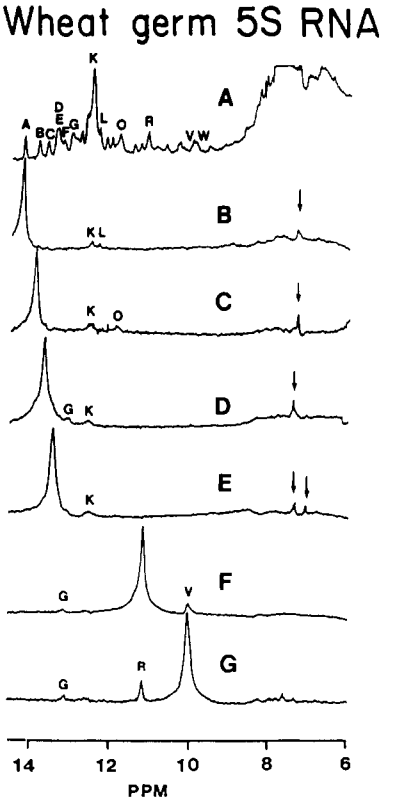

FIGURE 5: Identification of base-pair types from intact wheat germ 5S RNA via proton homonuclear Overhauser enhancement difference spectra. Presaturation of peaks A–E (spectra B–E) gives sharp NOE's between 7.0 and 7.5 ppm (see arrows), identifying resonances A–E as A·U base-pair hydrogen-bond imino protons. Note that the two distinct NOE's in plot E reveal that there are two A·U's at the position labeled D and E in the normal ^1H NMR spectrum (plot A). Presaturation of either peak R or peak V (spectra F and G) gave a strong mutual NOE to the other, identifying R and V as the two hydrogen-bond imino protons from a G·U pair. Various smaller NOE's (e.g., K and L in plot B) represent NOE connectivity to nearest-neighbor base pairs (see text).

different conformers may display more than one chemical shift. We are thus led to seek methods which can establish the number of distinct base pair protons for an envelope of overlapping resonances.

Resolution of Overlapping Peaks via Change in Salt Concentration. Magnesium ions bound to tRNA (Privalov & Filimonov, 1978) or wheat germ 5S RNA (Li & Marshall, 1985) are known to stabilize the RNA secondary and tertiary structures significantly. Figure 4 shows that wheat germ 5S RNA exhibits different configurations under different salt conditions, as evidenced by major shifts in the positions of the ^1H NMR peaks corresponding to hydrogen-bond base-pair imino protons. In particular, peaks D and E, unresolved in the *presence* of Mg^{2+} (Figure 4B) or Mg^{2+} and Na^+ (Figure 4A), split into two easily resolved peaks on removal of Mg^{2+} and Na^+ (Figure 4C). [Spectra at intermediate salt concentrations (not shown) confirm these and other assignments.] Similarly, the resonances at position K, which are unresolved in the *absence* of Na^+ and Mg^{2+} (Figure 4C), split into two major peaks on addition of either Mg^{2+} (Figure 4B) of Mg^{2+} and Na^+ (Figure 4A). Additional Mg^{2+}-induced changes are seen for the peaks located between 10 and 12 ppm. It is clear that variation in Na^+ and/or Mg^{2+} concentration produces differential chemical shifts for the hydrogen-bond base-pair imino protons, thereby furnishing a means for separating overlapping resonances. Once these resonances are identified and assigned, such spectra will report the site(s) of specific conformational changes induced by changes in salt concentrations.

Peak Identification (A·U, G·C, G·U) from NOE Pattern. One of the most useful NMR methods for identifying the number and type (e.g., A·U, G·C, G·U) is based upon the homonuclear Overhauser enhancement (NOE) technique. Partial transfer of a nonequilibrium population difference from an irradiated proton resoance to the spin populations of a spatially proximal (≤4 Å) proton causes a small decrease (for a molecule as large as 5S RNA) in the intensity of the dipole-coupled proton resonance (Noggle & Schirmer, 1971; Bothner-by, 1979). The difference is most readily visualized from the "NOE difference spectrum" obtained by subtracting the spectrum obtained during on-resonance irradiation from a spectrum obtained during off-resonance irradiation. The NOE difference spectral pattern will thus characterize the spatial distribution of protons in the close vicinity of the proton whose resonance is irradiated.

In particular, presaturation of an A·U base-pair proton (ca. 13.5–14.3 ppm) produces a characteristically sharp and strong NOE in the aromatic region (ca. 7.5 ppm) arising from coupling to the C2 proton of adenine in that base pair (Johnston & Redfield, 1981). Plots B–D of Figure 5 show that the three left-most peaks in the ^1H downfield NMR spectrum of wheat germ 5S RNA arise from A·U hydrogen-bond base-pair imino protons, as might have been guessed from their chemical shifts. The identification of peaks D, E offers a good example of the need for multiple experiments to test NMR-based inferences. First, the resonances at D, E appear more intense than those at A, B, and C (Figure 3), suggesting the presence of two base-pair protons. Accordingly, removal of Na^+ and Mg^{2+} (compare plots A or B with plot C of Figure 4) shows that peaks D, E indeed represent two different base-pair protons whose chemical shifts happen to overlap when salt is present. Finally, the NOE experiment (Figure 5, plot E) further reveals that the two peaks at D, E (Figure 5, plot A) are both A·U's, as seen from the two sharp NOE's generated in the aromatic region on irradiation of peaks D, E.

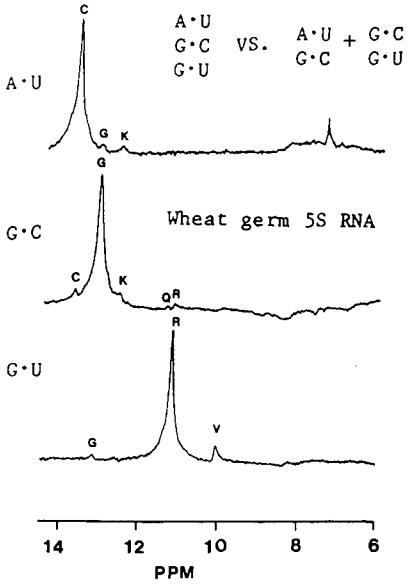

FIGURE 6: Ambiguity of NOE connectivity when overlapping resonances occur. Peaks C, G, and R are identified as A·U, G·C, and G·U from their characteristic primary NOE patterns. The top spectra show that A·U is adjacent to G·C, and the bottom spectrum shows that G·C is adjacent to G·U. However, since peak G represents two resonances (see 35 °C spectrum in Figure 7), we cannot be sure that the G·C connected to the A·U is the same G·C that is connected to G·U.

The G·U wobble base pair was the first to be identified (Johnson & Redfield, 1978: Roy & Redfield, 1981) from the strong mutual intrabase NOE's produced between the spatially close (2.5 Å) G-N1H and U-N3H. A typical G·U NOE pattern is observed for peaks R and V of Figure 3 (see Figure 5, plots F and G), providing immediate identification of R and V as the two hydrogen-bond imino protons of a G·U base pair.

Base-Paired Segments Determined by NOE Connectivity. The small (ca. 2–4%) NOE difference peaks arising from population transfer from an irradiated base-pair proton to a proton of the base pair immediately above or below it in an RNA helix can be used to identify adjacent base pairs. For example, Figure 5 (plot D) shows that resonance C (an A·U base-pair proton) is NOE-connected to resonance G (a G·C base-pair proton; see below). Similarly, resonances R and V (G·U base-pair protons from the same base pair) are NOE-connected to resonance G (Figure 5, plots F and G). A series of such 2-fold connections can be used to sequence longer helical base-paired segments of tRNA's and DNAs in solution (Heerschap et al., 1983a–c; Roy & Redfield, 1983; Hare & Reid, 1982; Feigon et al., 1983; Scheek et al., 1984). However, extension of the method to 5S RNAs presents new problems (Chang & Marshall, 1986). First, the secondary and tertiary structures of tRNA were already known (Ladner et al., 1975; Susman & Kim, 1976) in advance of the NMR work, whereas the 5S secondary structure (if a unique structure exists) is still debatable (Fox & Woese, 1975; Luoma & Marshall, 1978a,b; Studnicka et al., 1981; Nishikawa & Takemura, 1979; Delihas & Andersen, 1982; de Wachter et al., 1982); tertiary 5S RNA models are basically guesswork. Second, because 5S RNA is 1.5 times bigger than tRNA, there will be more peaks of greater individual line width, exagerating the problem of peak overlap, and the same weight per volume concentration will yield a 50% lower signal to noise ratio for 5S RNA compared to tRNA.

Suppose we now try to construct a base-pair sequence from NOE connectivities. Resonance C (Figure 6, top) is an A·U base-pair proton and is NOE-connected to resonances G and

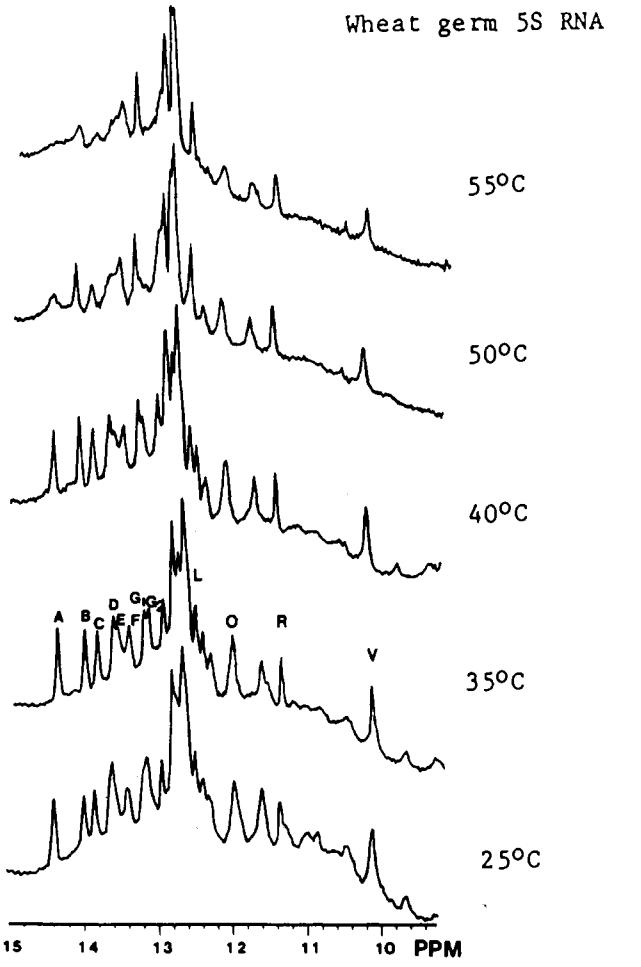

FIGURE 7: Use of temperature-induced melting and shifts to identify and confirm base-pair sequences in intact wheat germ 5S RNA (buffer A). Peaks A and L melt together, in agreement with their NOE connectivity (Figure 5, plot B). Note that peaks G splits into two peaks as the temperature is increased from 25 to 35 °C. Moreover, peak G_2 melts together with its NOE-connected peak C. On the other hand, peak G_1 is still intact at 55 °C, as are peaks R and V from a G·U base pair (see Figure 4, plots F and G). Peaks B and O are more stable than peaks A or C. Temperature variation experiments thus verify NOE connectivities and help to distinguish different NOE-connected segments.

K. The chemical shift and broad aromatic NOE produced by irradiation of peak G (Figure 6, middle) or peak K (not shown) identify both as G·C's. Figure 6 shows that peak G is NOE-connected to peaks C and R, V (and Q and possibly K). Finally, peaks R and V (Figure 6, bottom) are clearly from the same G·U, as argued previously. We have thus established NOE connectivity from peak K to peak C to peak G and from peak G to peaks R, V, corresponding to base-pair sequences G·C-A·U-G·C and G·C-G·U, respectively. (The polarity of each base pair, e.g., G·C vs. C·G, cannot be determined from these measurements.) One might be tempted to propose the completely connected sequence K-C-G-R, V, corresponding to G·C-A·U-G·C-G·U. However, the strong intensity of peak G suggests that it may contain more than one base-pair proton. Thus, we cannot be sure that the G·C (peak G) adjacent to an A·U (peak C) is the same G·C that is adjacent to a G·U (peaks R, V). This point is readily resolved from the temperature dependence of the ^{1}H NMR spectrum, as discussed next.

Temperature-Induced Shifts and Melting as an Aid in Base-Pair Sequencing. Temperature-induced changes in the ^{1}H NMR spectrum of 0.75 mM wheat germ 5S RNA in buffer A are shown in Figure 7, obtained with a General

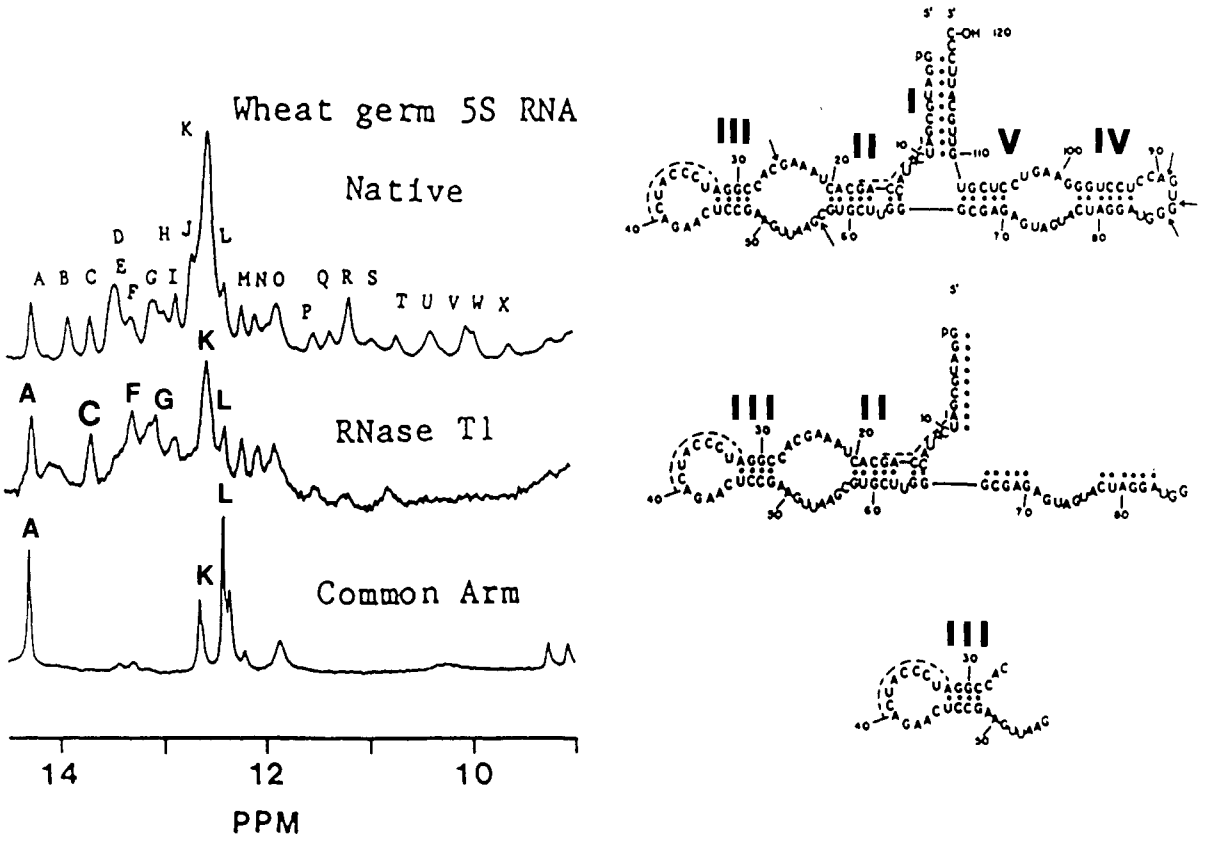

FIGURE 8: Proton 500-MHz NMR spectra (left) and proposed secondary structures (right) of intact wheat germ 5S RNA (top) and two purified fragments (middle and bottom) produced by RNase T1 cleavage. All samples are in buffer B. The most obvious results of RNase T1 cleavage are the elimination of three A·U base pairs (peaks B, D, and E) and one G·U (peaks R and V).

Electric NT-500 FT/NMR spectrometer. Since two NOE-connected base-pair proton peaks presumably occupy adjacent rungs of an RNA A-helix, both base pairs should "melt" (i.e., the inverse lifetime for chemical exchange between the base-pair proton and H_2O becomes faster than about 30 s^{-1}) at about the same temperature. For example, peaks A and L (whose NOE connectivity is shown in Figure 5B) melt together at about 50 °C.

Let us now consider the problem of the overlapped G·C resonances at position G. Two G·C resonances, G_1 and G_2, are clearly resolved when the temperature is increased to 35 °C (or in the buffer of Figure 4A). Peak G_2 melts together with peak C (an A·U pair) at about 50 °C. However, peaks R and V (a G·U pair) remain stable up to 55 °C, along with peak G_1. Thus, it is likely that the G·C (peak G_2) which is adjacent to an A·U (peak C) is different from the G·C (peak G_1) which is adjacent to a G·U (peaks R, V). The corresponding base-paired segments, G·C-A·U-G·C (peaks K-C-G_2) and G·C-G·U (peaks G_1-R, V), likely occur in different base-paired helical stems. (It is important to note that a common melting temperature for a G·C pair and an A·U pair need not imply a common location, since an A·U pair may melt at a lower temperature than an adjacent G·C pair.)

Although G·U base pairs have generally been regarded as much weaker than A·U or G·C pairs (Tinoco et al., 1973), Johnston and Redfield (1978) demonstrated the persistence of G4·U69 in $tRNA^{Phe}$ up to 42 °C in the presence of Mg^{2+}. Similarly, we find a G·U base pair (peaks R, V) that is as stable at high temperature as the remaining G·C pairs near 12.5 ppm (see 55 °C spectrum in Figure 7). The stem containing the G·C-G·U segment must be stabilized by the presence of other secondary G·C pairs or additional tertiary base pairing.

Finally, peaks B (A·U pair) and O, whose NOE connectivity is shown in Figure 5C, are both also stable at high temperature (see 50 °C spectrum of Figure 7). In contrast, the A·U base-pair protons corresponding to peaks A and C are relatively labile and likely occur in less stable regions [e.g., helix II or helix III of the Fox/Woese model (see below)].

Use of RNase T1 Cleavage Fragments for Assignment of Base-Paired Segments. Although the resonances corresponding to five A·U and one G·U base pairs have been identified (Figure 5), and their NOE connectivities established (Figures 5–7), assignment of particular resonances to particular primary sequence positions in wheat germ 5S RNA remains. For example, the base-pair sequence G·C-A·U-G·C deduced from NOE connectivity between resonances K-C-G_2 could be assigned to two possible segments in the Fox and Woese model, namely, $C_{18}G_{60}$-$A_{19}U_{59}$-$C_{20}G_{58}$ and $C_{105}G_{70}$-$U_{106}A_{69}$-$C_{107}G_{68}$.

A simple method for resolving such an issue is to cleave the intact 5S RNA molecule in such a way to eliminate one possible helical segment while preserving another. Figure 8 shows ^1H NMR spectra and corresponding secondary structures (Fox/Woese model) of intact wheat germ 5S RNA, an RNase T1 resistant cleavage fragment, and a smaller fragment corresponding to the "common arm" that is present in virtually all proposed secondary structures for 5S RNA.

Figure 8 shows that peaks B (A·U), D (A·U), E (A·U), and R, V (G·U) are missing in the RNase T1 resistant cleavage fragment and thus appear to arise from segments I, IV, and/or V (and/or from tertiary base pairs). By the same token, since peaks A and C remain after RNase T1 cleavage, we discover that peaks A (A·U) and C (A·U) and their NOE-connected partners are found in helices II and III. Further cleavage of the RNase T1 resistant fragment (S.-J. Li and A. G. Marshall,

Table I: Comparison of Experimental ^1H NMR Chemical Shifts with Those Computed from Ring Currents for a Proposed Base-Pair Sequence

peak position[a]	base pair	calcd shift[b] (ppm)	exptl shift (ppm)
K	C_{18}·G_{60}	12.49	12.53
C	A_{19}·U_{59}	13.80	13.64
G_2	C_{20}·G_{58}	13.24	13.11

[a] See Figure 2. [b] Computed from Arter and Schmidt (1976) for an RNA A-helix, for assumed intrinsic (unshifted) positions of 14.35 ppm for A·U and 13.45 ppm for G·C (Reid et al., 1979).

unpublished results) was used to produce the common arm segment shown in Figure 8 (bottom). Since peak A remains in the spectrum of the common arm fragment, we have detected at least one A·U base pair from the common arm. Similarly, since peak C is missing from the common arm segment, we conclude that peak C lies in helix II and is assigned to $A_{19}U_{59}$. Therefore, NOE-connected resonances K-C-G_2 can be assigned to $C_{18}G_{60}$-$A_{19}U_{59}$-$C_{20}G_{58}$ and *constitute the first direct observation of the "tuned" helix II segment of the Fox/Woese secondary strcutural model for 5S RNA.*

Ring Current Induced Chemical Shifts Confirm Assignment of $C_{18}G_{60}$-$A_{19}U_{59}$-$C_{20}G_{59}$. Further corroboration of the assignment of peaks K-C-G_2 as $C_{18}G_{60}$-$A_{19}U_{59}$-$C_{20}G_{58}$ is afforded from ring current calculations. Table I compares the experimental chemical shifts for peaks G_2, C, and K with those computed from Arter and Schmidt (1976) for nearest and next-nearest base pairs in the tuned helix II of the Fox/Woese model. The calculated values are clearly consistent with the proposed assignment. In conclusion, a combination of proton homonuclear NOE experiments, variation of salt conditions, temperature-induced melting, and ^1H NMR of RNase T1 enzymatic cleavage fragments yields a relatively definitive assignment of a segment of base pairs that can be assigned to the previously unobserved tuned helix II region of the Fox/Woese model of the secondary structure of wheat germ 5S RNA.

Are the Conformations of the Fragments the Same as in the Intact Molecule? It is important to establish that the enzymatic cleavage fragments differ from the intact 5S RNA molecule only in the absence of some structural features and not by the formation of some new, nonnative structure. Since the principal difference between the fragments and the intact molecule is that several resonances are absent in the fragments, it seems likely that the base-paired regions of the fragments are similar to those in the intact 5S RNA. [Some minor additional peaks observed for the fragment (e.g., extra intensity at 14.1 ppm) could arise from pairing of the long loose 5′ and 3′ends.] A better criterion is to compare the NOE behavior of the fragment and the intact 5S RNAs. Figure 9 shows that irradiation of peak C in the RNase T1 resistant cleavage fragment produces an NOE pattern nearly identical with that from the intact 5S RNA (Figure 5D or Figure 6, top spectrum). As further evidence, Figure 10 shows NOE patterns for irradiation of peak A from the intact molecule (bottom spectrum), the RNase T1 resistant fragment (middle spectrum), and the common arm fragment (top spectrum). The near-identical NOE pattern for all three RNAs offers strong evidence that the conformation of the fragments is similar to the conformation of the corresponding segments of the intact wheat germ 5S RNA. [The slight shift in position of peak A in the common arm fragment compared to the other fragment and the intact 5S RNA is due to the lower temperature

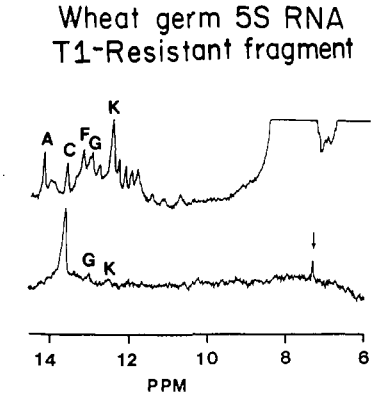

FIGURE 9: Presaturation of peak C on the RNase T1 resistant fragment shown in the middle of Figure 8 gave the same NOE pattern (bottom spectrum) as for the intact molecule (compare spectrum D in Figure 4). The spectrum of the fragment (top diagram) is included for reference. This result supports the assumption that the fragment retains at least some of the features of the intact 5S RNA molecule.

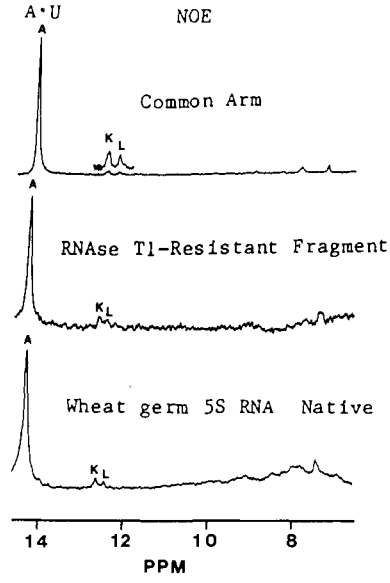

FIGURE 10: Same NOE pattern is produced by irradiation of the A·U resonance at peak A, whether from intact 5S RNA (bottom), the RNase T1 resistant fragment (middle), or the common arm fragment (top), indicating that this segment of the molecule survives intact after RNase T1 cleavage.

(2 vs. 23 °C) at which the NOE of the common arm fragment was conducted.]

5S RNA Secondary Structure. The secondary structures of ribosomal 5S RNA (Eigen et al., 1985; Curtiss & Vournakis, 1984; Ohama et al., 1984; Delihas et al., 1984; Pieler et al., 1984) and 5.8S RNA (Vaughn et al., 1984) have been repeatedly and extensively reviewed. Although there are minor differences between recent models with respect to length of helical segments and the disposition of single-stranded loops or bulges, most are characterized by a three-stem arrangement (including four helical segments for prokaryotes and five for eukaryotes), except for the cloverleaf model (Luoma & Marshall, 1978a,b) which has four stems. The two model types have been adapted to the primary base sequence of wheat germ 5S RNA in Figure 1.

The major difference between the two models is the base-pairing arrangement in the middle of the primary sequence, i.e., helices II and III in the three-stem model or the single helix AA′ in the four-stem cloverleaf model. As previously noted, the present results require a G·C-A·U-G·C base-pair sequence both in the intact 5S RNA and in the RNase T1

resistant cleavage fragment. However, no such base-pair arrangement can be found in the cloverleaf model. Moreover, stem A of the cloverleaf model includes three G·U pairs, but no G·U base-pair protons are NOE observable in the corresponding RNase T1 resistant cleavage fragment. On the other hand, NOE-connectivity and ring current calculations support $C_{18}G_{60}$-$A_{19}U_{59}$-$C_{20}G_{58}$ assignment to the tuned helix II of the three-stem model. The alternative $G_{68}C_{107}$-$A_{69}U_{106}$-$G_{70}C_{105}$ segment in helix V is ruled out by the continued presence of the signals in the RNase T1 resistant cleavage fragment, in which bases 90–120 have been removed. The experimental absence of G·U pairs in the RNase T1 resistant cleavage fragment further supports the existence of helix II, in which no G·U's are present. The present results thus provide the most direct evidence to date for the existence of the tuned helix II and thus strongly support a three-stem secondary structural model for 5S RNA.

The exact number of base pairs in helix II remains to be determined. First, RNase S_1 cleavage of positions 8–18 (Barber & Nichols, 1978) indicates that helix II may not contain as many as five consecutive base pairs. Second, we do not detect an A·U base pair corresponding to $A_{16}U_{62}$ in the ^{1}H NMR spectrum of either the intact molecule or the RNase T1 resistant cleavage fragment (even with NOE's at 5 °C), although a shoulder at the left of peak F could represent such a base pair whose hydrogen-bond imino proton is in fast exchange with water because of its location at the end of a helical segment. Furthermore, a few resonances remain after subtraction of the common arm resonances and the assigned peaks G_2, C, and K from the RNase T1 resistant cleavage fragment spectrum, suggesting that the revised Fox/Woese model is incomplete. Although there are no less than five G·U base pairs in the secondary structure of intact wheat germ 5S RNA, only one or two G·U's are observed by ^{1}H NOE experiments. This anomaly may be explained by overlap of peaks at positions R, V, and possibly W, absence of G·U pairs from the actual secondary structure, or high lability for chemical exchange for the remaining G·U pairs, so that their NMR signals are too broad for us to see, even at 2 °C.

Limitations of the NOE Method and Implications for Future Work. Base-pair sequences constructed from NOE connectivities have been quite accurate for tRNA solution structures (Johnston & Redfield, 1981; Hare & Reid, 1982; Heerschap et al., 1983a,b) and for some small DNAs (Hare et al., 1983; Scheek et al., 1984). The principal limiation of the method occurs when two or more peaks overlap, as in peak K in Figure 3. Peak K contains approximately 8–10 resonances, as judged from its relative intensity and from the temperature-induced melting profiles in Figure 7. Thus, a base-paired segment inferred from NOE connectivity ends when one of the resonances in peak K is involved (see Figure 5B–E); irradiation at peak K gives too many possible neighbor base pairs to choose the next neighbor in the segment. For example, if peak K contains 8 resonances, then there could be as many as 16 NOE connections from base pairs above and below the base pairs whose protons all share the same chemical shift at K, making base-pair sequence assignments highly ambiguous. Moreover, because peak K is so large, even a small degree of spillover of decoupler power from irradiation of a nearby peak can contribute an NOE difference peak at K, whether the K protons are dipole coupled to the irradiated peak or not—Figure 5E could present such a case.

From the appearance of two aromatic peaks in the NOE difference spectrum, and by variation of buffer conditions, we conclude that the overlapping resonances labeled D, E must represent hydrogen-bond imino protons from two different A·U base pairs. On the basis of their disappearance from the spectrum of the RNase T1 resistant cleavage fragment, D, E might be A_3U_{116} and U_4A_{115}. Although the two resonances are slightly separated when Na^+ are removed (Figure 4, bottom), direct irradiation of either peak will produce a small difference peak at the other resonance position due to spillover of the presaturation power. A possible solution of this problem would be to employ a two-dimensional NOE experiment (NOESY) (Haasnoot et al., 1983), although such experiments become quite difficult for spectra with peaks with 50-Hz line widths.

Finally, it is important to recognize that NOE experiments detect protons that are spatially close to the proton whose resonance is irradiated. In particular, secondary base pairs cannot be distinguished from tertiary base pairs. Thus, it is possible to infer an incorrect secondary base-pair sequence if one of the base pairs happens to be a tertiary rather than a secondary pair.

Because of the above problems, NOE experiments must be supported by other procedures which shift or simplify the ^{1}H NMR spectrum: use of enzymatic cleavage fragments (Kime & Moore, 1983a,b; this work), variation in temperature, change in salt conditions, site-specific spin-labeling (K. M. Lee and A. G. Marshall, unpublished results), comparison of spectra from 5S RNA from organisms whose 5S RNAs differ in only a few primary positions (S.-M. Chen and A. G. Marshall, unpublished results), deuterium exchange (K. M. Lee and A. G. Marshall, unpublished results), etc. For wheat germ 5S RNA, several other RNase T1 fragments designed to isolate other secondary structural segments are presently under investigation in our laboratory.

Acknowledgments

We thank C. E. Cottrell, L.-H. Chang, S.-M. Chen, and T.-C. Lin Wang for valuable discussions and assistance. We also thank International Multifoods, Columbus, OH, for their generous donation of wheat germ.

Registry No. Na, 7440-23-5; Mg, 7439-95-4.

References

Arter, D. B., & Schmidt, P. G. (1976) *Nucleic Acids Res. 3*, 1437–1447.

Barber, C., & Nichols, J. L. (1978) *Can. J. Biochem. 56*, 357–364.

Bellemare, G., Vigne, R., & Jordan, B. (1973) *Biochimie 55*, 29–35.

Bothner-By, A. A. (1979) in *Biological Applications of Magnetic Resonance* (Shulman, R. G., Ed.) pp 177–219, Academic Press, New York.

Brownlee, G. G., Sanger, F., & Barrell, B. G. (1967) *Nature (London) 215*, 735.

Burkey, K. O., Marshall, A. G., & Alben, J. O. (1983) *Biochemistry 22*, 4223–4229.

Burns, P. D., Luoma, G. A., & Marshall, A. G. (1980) *Biochem. Biophys. Res. Commun. 96*, 805–811.

Chang, L.-H., & Marshall, A. G. (1986) *Biochemistry 25*, 3056–3063.

Chang, L.-H., Burkey, K. O., Alben, J. O., & Marshall, A. G. (1984) *Biochemistry 23*, 3659–3662.

Curtiss, W. C., & Vournakis, J. N. (1984) *J. Mol. Evol. 20*, 351–361.

Delihas, N., & Andersen, J. (1982) *Nucleic Acids Res. 10*, 7323–7344.

Delihas, N., Andersen, J., & Singhal, R. P. (1984) *Prog. Nucleic Acid Res. Mol. Biol. 31*, 161–190.

De Wachter, R., Chen, M.-W., & Vandenberghe, A. (1982) *Biochimie 64*, 311–329.

Eigen, M., Lindemann, B., Winkler-Oswatitsch, R., & Clarke, C. H. (1985) *Proc. Natl. Acad. Sci. U.S.A. 82*, 2437–2441.

Erdmann, V. A. (1976) *Prog. Nucleic Acid Res. Mol. Biol. 18*, 45–90.

Erdmann, V. A., Wolters, J., Huysmans, E., & De Wachter, R. (1985) *Nucleic Acids Res. 13*, r105–r153.

Fox, G. E., & Woese, C. R. (1975) *Nature (London) 256*, 505–507.

Haasnoot, C. A. G., Den Hartoy, J. H. J., De Rooy, F. M., Van Boom, J. H., & Altona, C. (1980) *Nucleic Acids Res. 8*, 169–181.

Haasnoot, C. A. G., Heerschap, A., & Hilbers, C. W. (1983) *J. Am. Chem. Soc. 105*, 5483–5484.

Hare, D. R., & Reid, B. R. (1982) *Biochemistry 21*, 5129–5135.

Hare, D. R., Wemmer, D. E., Chou, S.-H., Drobny, G., & Reid, B. R. (1983) *J. Mol. Biol. 171*, 319–336.

Heerschap, A., Haasnoot, C. A. G., & Hilbers, C. W. (1982) *Nucleic Acids Res. 10*, 6981–7000.

Heerschap, A., Haasnoot, C. A. G., & Hilbers, C. W. (1983a) *Nucleic Acids Res. 11*, 4483–4499.

Heerschap, A., Haasnoot, C. A. G., & Hilbers, C. W. (1983b) *Nucleic Acids Res. 11*, 4501–4520.

Holley, R. W., Apgar, J., Everett, G. A., Madison, J. T., Marquisee, M., Merrill, S. H., Penswick, J. R., & Zamir, A. (1965) *Science (Washington, D.C.) 147*, 1462–1465.

Johnston, P. D., & Redfield, A. G. (1978) *Nucleic Acids Res. 5*, 3913–3927.

Johnston, P. D., & Redfield, A. G. (1981) *Biochemistry 20*, 1147–1156.

Jordan, B. R. (1971) *J. Mol. Biol. 55*, 423.

Kearns, D. R., Patel, D., & Shulman, R. G. (1971a) *Nature (London) 229*, 338–339.

Kearns, D. R., Patel, D., Shulman, R. G., & Yamane, T. (1971b) *J. Mol. Biol. 61*, 265–270.

Kime, M. J. (1984a) *FEBS Lett. 173*, 342–346.

Kime, M. J. (1984b) *FEBS Lett. 175*, 259–262.

Kime, M. J., & Moore, P. B. (1983a) *Biochemistry 22*, 2615–2622.

Kime, M. J., & Moore, P. B. (1983b) *Biochemistry 22*, 2622–2629.

Kime, M. J., Gewirth, D. T., & Moore, P. B. (1984) *Biochemistry 23*, 3559–3568.

Ladner, J. E., Jack, A., Robertus, J. D., Brown, R. S., Rhodes, D., Clark, B. F. C., & Klug, A. (1975) *Proc. Natl. Acad. Sci. U.S.A. 72*, 4414–4418.

Lewis, J. B., & Doty, P. (1970) *Nature (London) 225*, 510.

Li, S.-J., & Marshall, A. G. (1985) *Biochemistry 24*, 4047–4052.

Li, S.-J., Chang, L.-H., Chen, S.-M., & Marshall, A. G. (1984a) *Anal. Biochem. 138*, 465–471.

Li, S.-J., Burkey, K. O., Luoma, G. A., Alben, J. O., & Marshall, A. G. (1984b) *Biochemistry 23*, 3652–3658.

Leuhrsen, K. R., & Fox, G. E. (1981) *Proc. Natl. Acad. Sci. U.S.A. 78*, 2150–2154.

Luoma, G. A., & Marshall, A. G. (1978a) *Proc. Natl. Acad. Sci. U.S.A. 75*, 4901–4905.

Luoma, G. A., & Marshall, A. G. (1978b) *J. Mol. Biol. 125*, 95–105.

Mackay, R. M., Spencer, D. F., Doolittle, W. F., & Gray, M. W. (1980) *Eur. J. Biochem. 112*, 561–576.

Mackay, R. M., Spencer, D. F., Schnare, N. N., Doolittle, W. F., & Gray, M. W. (1982) *Can. J. Biochem. 60*, 480–489.

Matveev, S. V., Filimonov, V. V., & Privalov, P. L. (1982) *Mol. Biol. (Engl. Transl.) 16*, 990–999.

Nishikawa, K., & Takemura, S. (1974) *J. Biochem. (Tokyo) 76*, 935–947.

Noggle, J. H., & Schirmer, R. E. (1971) *The Nuclear Overhauser Effect: Chemical Applications*, Academic Press, New York.

Ohama, T., Kumazaki, T., Hori, H., & Osawa, S. (1984) *Nucleic Acids Res. 12*, 5101–5108.

Osterberg, R., Sjoberg, B., & Garrett, R. A. (1976) *Eur. J. Biochem. 68*, 481–487.

Pace, B., Matthews, E. A., Johnson, K. D., Cantor, C. R., & Pace, N. R. (1982) *Proc. Natl. Acad. Sci. U.S.A. 79*, 36–40.

Peattie, D. A., & Gibert, W. (1980) *Proc. Natl. Acad. Sci. U.S.A. 77*, 4679–4682.

Pieler, T., & Erdmann, V. A. (1982) *Proc. Natl. Acad. Sci. U.S.A. 79*, 4599–4603.

Pieler, T., Digweed, M., & Erdmann, V. A. (1984) in *Gene Expression* (Clark, B. F. C., & Petersen, H. U., Eds) pp 353–376, Munksgaard, Copenhagen.

Privalov, P. L., & Filimonov. V. V. (1978) *J. Mol. Biol. 122*, 447–464.

Raiford, D. S., Fisk. C. L., & Becker, E. D. (1979) *Anal. Chem. 51*, 2050–2051.

Redfield, A. G., & Kunz, S. D. (1979) in *NMR and Biochemistry* (Opella, S. J., & Lu, P., Eds.) pp 225–239, Marcel Dekker, New York.

Redfield, A. G., Kunz, S. D., & Palph, E. K. (1975) *J. Magn. Reson. 19*, 114–117.

Reid, B. R., McCollum, L., Ribeiro, N. S., Abbate, J., & Hurd, R. E. (1979) *Biochemistry 18*, 3996–4005.

Ross, A., & Brimacombe, R. (1979) *Nature (London) 281*, 271–276.

Roth, K., Kimber, B. J., & Feeney, J. (1980) *J. Magn. Reson. 41*, 302–309.

Roy, S., & Redfield, A. g. (1981) *Nucleic Acids Res. 9*, 7073–7083.

Roy, S., & Redfield, A. G. (1983) *Biochemistry 22*, 1386–1390.

Salemink, P. J. M., Raue, H. A., Heerschap, A., Plant, R. J., & Hilbers, C. W. (1981) *Biochemistry 20*, 265–272.

Scheek, R. M., Boelens, R., Russo, N., van Boom, J. H., & Kaptein, T. (1984) *Biochemistry 23*, 1371–1376.

Schimidt, P. G., & Kastrup, R. V. (1978) in *Biomolecular Structure and Function* (Agris, P., Ed.) pp 517–525, Academic Press, New York.

Schimmel, P. R., & Redfield, A. G. (1980) *Annu. Rev. Biophys. Bioeng. 9*, 181–221.

Soot, M. B., Saarma, R. L., Willems, E., Lind, A. J., & Vasilenko, S. K. (1974) *Mol. Biol. (Engl. Transl.) 8*, 723.

Studnicka, G. M., Eiserling, F. A., & Lake, J. A. (1981) *Nucleic Acids Res. 9*, 1885–1904.

Sussman, J. L., & Kim, S.-H. (1976) *Biochem. Biophys. Res. Commun. 68*, 89–96.

Tinoco, I., Borer, P. N., Dengler, B., Levine, M. D., Uhlenbeck, O. C., Crothers, D. M., & Gralla, J. (1973) *Nature (London), New Biol. 146*, 40–41.

van Geet, A. L. (1970) *Anal. Chem. 42*, 679–680.

Vaughn, J. C., Sperbeck, S. J., Ramsey, W. J., & Lawrence, C. B. (1984) *Nucleic Acids Res. 12*, 7479–7502.
Vigne, R., Jordan, B. R., & Monier, R. (1973) *J. Mol. Biol. 76*, 303–311.
Woese, E. R., Magrum, L. J., Gupta, R., Siegel, R. B., & Stahl, D. A. (1980) *Nucleic Acids Res. 8*, 2275–2293.
Wong, Y. P., Kearns, D. R., Reid, B. R., & Shulman, R. G. (1972) *J. Mol. Biol. 72*, 741–749.
Wrede, P., & Erdmann, V. A. (1973) *FEBS Lett. 33*, 315–319.
Zagorska, L., Duin, J. V., Noller, H. F., Pace, B., Johnson, K. D., & Pace, N. R. (1984) *J. Biol. Chem. 259*, 2798–2802.

Binding of *Escherichia coli* Protein Synthesis Initiation Factor IF1 to 30S Ribosomal Subunits Measured by Fluorescence Polarization†

Frank H. Zucker‡ and John W. B. Hershey*
Department of Biological Chemistry, School of Medicine, University of California, Davis, California 95616
Received September 17, 1985; Revised Manuscript Received February 5, 1986

ABSTRACT: The interaction of initiation factor IF1 with 30S ribosomal subunits was measured quantitatively by fluorescence polarization. Purified IF1 was treated with 2-iminothiolane and *N*-[[(iodoacetyl)amino]ethyl]-5-naphthylamine-1-sulfonic acid in order to prepare a covalent fluorescent derivative without eliminating positive charges on the protein required for biochemical activity. The fluorescent-labeled IF1 binds to 30S subunits and promotes the formation of *N*-formylmethionyl-tRNA complexes with 70S ribosomes. Analyses of mixtures of fluorescent-labeled IF1 and 30S ribosomal subunits with an SLM 4800 spectrofluorometer showed little change in fluorescence spectra or lifetimes upon binding, but a difference in polarization between free and bound forms is measurable. Bound to free ratios were calculated from polarization data and used in Scatchard plots to determine equilibrium binding constants and number of binding sites per ribosomal subunit. Competition between derivatized and nonderivatized forms of IF1 was quantified, and association constants for the native factor were determined: $(5 \pm 1) \times 10^5$ M^{-1} with IF1 alone; $(3.6 \pm 0.4) \times 10^7$ M^{-1} with IF3; $(1.1 \pm 0.2) \times 10^8$ M^{-1} with IF2; $(2.5 \pm 0.5) \times 10^8$ M^{-1} with both IF2 and IF3. In all cases, 0.9–1.1 binding sites per 30S subunit were detected. Divalent cations have little effect on affinities, whereas increasing monovalent cations inhibit binding. On the basis of the association constants, we predict that greater than 90% of native 30S subunits are complexed with all three initiation factors in intact bacterial cells.

During initiation of protein synthesis in bacteria, the 70S ribosome dissociates into subunits, the 30S subunit forms a preinitiation complex with *N*-formylmethionyl-tRNA ($fMet\text{-}tRNA_f$)[1] and mRNA, and the 50S subunit joins the preinitiaton complex to form a 70S initiation complex capable of entering the elongation phase [for reviews, see Maitra et al. (1982) and Grunberg-Manago et al. (1978)]. This process is promoted by three initiation factors: IF1 (M_r 8119), IF2 (M_r 97 300 and 79 700) and IF3 (M_r 20 668). IF3 helps dissociate ribosomes and is associated with mRNA binding. IF2 is involved with fMet-tRNA binding and hydrolyzes GTP. IF1 stimulates the rate of ribosome dissociation and generally assists in the actions of the other two factors. In spite of extensive efforts over the past 15 years, the detailed molecular mechanisms of action of the initiation factors remain unclear.

Elucidation of the pathway of initiation and of possible translational control mechanisms requires a detailed knowledge of the kinetic parameters for the various reactions involved. Studies of the rates of binding of fMet-tRNA and mRNA by membrane filtration (Gualerzi et al., 1977; van der Hofstad et al., 1978) and spectrophotometric (Wintermeyer & Gualerzi, 1983) techniques indicate that their binding may be either a random or an ordered process. We have focused on the interaction of the initiation factors with 30S subunits, initially using radiolabeled factors and sucrose density gradient centrifugation to monitor binding (Fakunding & Hershey, 1973; Heimark et al., 1976; Langberg et al., 1977). Whereas these studies showed that individually the stability of 30S binding is IF3 > IF2 > IF1, this method is unsuited to quantitative kinetic studies. More recently we used fluorescence polarization techniques to determine the equilibrium association constants (K_a) for 30S subunits and IF2 (Weiel & Hershey, 1982) and IF3 (Weiel & Hershey, 1981). Fluorescence polarization allows measurement of the binding of a small, covalently derivatized initiation factor with the relatively large 30S ribosomal subunit. The K_a for IF3 and 30S subunits is 3.1×10^7 M^{-1} and does not change appreciably in the presence of the other factors. The K_a for IF2 alone is 2.7×10^7 M^{-1} but increases to 1.8×10^8 M^{-1} in the presence of IF1 and IF3. In the work reported here, we prepared an active fluorescent derivative of IF1 and measured the K_a for IF1 and 30S subunits with and without the other factors. The

†This research was supported by Grant NP-70 from the American Cancer Society.
‡Present address: Fred Hutchinson Cancer Research Center, Seattle, WA 98104.

[1] Abbreviations: fMet-tRNA, *N*-formylmethionyl-tRNA; IF, initiation factor; PAGE, polyacrylamide gel electrophoresis; SDS, sodium dodecyl sulfate; NEPHGE, nonequilibrium pH gradient electrophoresis; BME, β-mercaptoethanol; TEA, triethanolamine; 2-ITL, 2-iminothiolane; F-IF1, fluorescent-labeled IF1; 1,5-IAEDANS, *N*-[[(iodoacetyl)amino]ethyl]-5-naphthylamine-1-sulfonic acid; Tris-HCl, tris(hydroxymethyl)aminomethane hydrochloride; EDTA, ethylenediaminetetraacetic acid.

0006-2960/86/0425-3682$01.50/0